PCR-free DNA-based biosensing with polymeric optical hybridization transduction using micro- and submicron-magnetic bead captured on micro-electromagnetic traps

Sébastien Dubus [1], Boris Le Drogoff [2],
Jean-François Gravel [1], Denis Boudreau [1] and Teodor Veres (presenting) [2]*

[1] Département de chimie et Centre d'Optique Photonique Laser (COPL)
Université Laval, Qc, G1K 7P4, Canada;
[2] Industrial Material Institute, National Research Council Canada
75, de Mortagne, Boucherville, Qc, J4B 6Y4, Canada
* E-mail : teodor.veres@cnrc-nrc.gc.ca, Phone: (450) 641-5232, Fax: (450) 641-5105

ABSTRACT

In this paper, we present results from an approach based on the rapid and selective capture of target nucleic acids grafted on probe-functionalized magnetic micro- and nanobeads using integrated micro-electromagnetic traps in a microfluidic platform, followed by real-time optical detection. The influence of the magnetic bead diameter, from 2.8-μm to 500-nm diameter beads, has been systematically investigated in term of particle mobility under magnetic field and fluorescence signal (S/N ratio). It is clearly shown that reducing the size of magnetic particles offers higher sensitivity for the optical detection but decreases the magnetic trapping efficiency and the dynamic range for the microfluidic flow. By optimizing both parameters, this technique allows the detection of a few hundred copies of bio-threat-specific DNA material in less than one hour without any chemical or enzymatic pre-amplification.

Keywords: DNA-based biosensor, magnetic particles, magnetic confinement, electro-magnetic traps, PCR-free sensibility, Lab-on-a-Chip.

1 INTRODUCTION

The interest in the development of fast and reliable sequence-specific DNA biosensors has grown tremendously over the past few years. Because the amount of DNA material to be detected is often extremely small, the need for a detection scheme capable of transducing the hybridization event with sufficient sensitivity has led to the investigation of a number of sensitive approaches.

A strategy that has increased in popularity in recent years is the use of surface-functionalized magnetic particles to selectively bind low-abundance target analytes (DNA, bacteria or viruses) in order to preconcentrate them prior to the detection step [1-2]. These particles are available across a wide size range and offer large contact surfaces for specific functionalization, thus allowing the optimization of and separation procedures with relative ease of use. While the most effective way to concentrate these particles is still the use of macroscopic permanent magnets, recent reports have shown the possibility to effectively manipulate and control the motion of magnetic microbeads on the micron scale [3-5]. This offer the possibility to concentrate, confine and detect targeted analytes in a microscopic volume using magnetically "tagged" probes and very sensitive optical methods.

Our approach uses magnetic microbeads functionalized with ssDNA probes and a fluorescent polymeric transducer that allow for the highly sensitive detection of target DNA without the need for any additional fluorescent DNA labelling [6]. This method involves three steps: 1) grafting the beads with a specific probe, 2) duplex formation on the beads' surface and 3) hybridization of target on beads and detection following magnetic confinement. We recently demonstrated that this technique can be used to detect target DNA directly on magnetic particles while the micro-beads are being magnetically confined in a small volume by a micro-electromagnetic trap (μEMT) [7-8].

In this work, two different geometries of micro-electromagnetic traps (μEMT) have been designed for the capture of functionalized magnetic beads on a microfluidic platform. A confocal fluorescence detection system has been used to perform "on-bead detection" at the center of the μEMT. A systematic investigation in terms of magnetic capture efficiency under magnetic field and hydrodynamic forces, and fluorescence signal as a function of bead size (from 2.8 μm to 500 nm) were performed.

2 EXPERIMENTAL

2.1 Fabrication of micro-electromagnetic trap devices

The first studied generation of μEMT consists of a planar micron-scale current-carrying gold conductor based on a circular design described by C.S. Lee *et al*. [5]. We recently improved this design by adding, in a second generation of μEMT, a nickel micropost in the middle of the loop in order to concentrate the magnetic field and thus the magnetic force in the center of the traps [9]. Our microfabrication process method can be divided as follow:

(i) a conducting seed layer of Cr was deposited (as an adhesion layer) followed by a layer of Au using an electron-beam evaporator; (ii) AZ-9260 photoresist was spun on the wafer to pattern, after UV exposure, an electroplating mold for the circular conductor shape as well as the contact pads; (iii) the mold was filled with 10 µm of electroplated gold and (iv) the non-electroplated area of the seed layer was etched away to complete the fabrication of the first generation of µEMT. Fig. 1a shows an electromagnetic ring trap at this stage of the microfabrication process. In order to fabricate the second generation of µEMT with a Ni micropost, the conductive seed layer was kept on the substrate and the process was repeated from step (ii) to step (iv), but this time the resist mold was filled with electroplated nickel (fig. 1b).
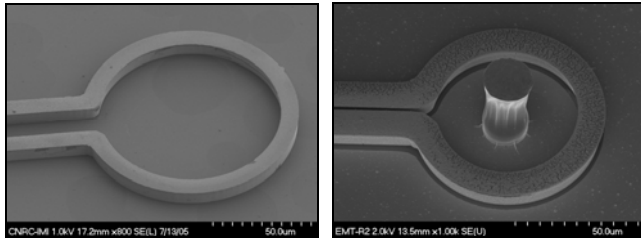

Fig. 1: SEM picture of a microfabricated electromagnetic trap: (a) first generation based on the design of Ref [5], (b) second generation with Ni micropost in the center.

Finally, to complete the microfabrication of functional device, a thin insulating layer of premixed poly(dimethylsiloxane) (PDMS) was spun on top of the µEMTs. In order to optimize the magnetic field profile, the thickness of this insulating layer was optimized by numerical simulations (see section 3.1).

Microfluidic PDMS channels were fabricated using a replica molding technique [10] and then aligned with the µEMT. Excellent sealing was obtained between the two PDMS layers. The liquid containing the magnetic particles was pumped into the microfluidic channel by using a syringe pump.

2.2 Materials and Chemistry

Superparamagnetic, streptavidin functionalized microbeads of various diameters were acquired from Dynal Biotech (2.8 and 1.0 µm) and Ademtech (500 nm).

Synthesized DNA samples were all obtained from Integrated DNA technologies, Inc., and TriLink Biotechnologies Inc. The polythiophene synthesis procedure has been described elsewhere [11]. Quantitative measurements performed with the polymeric transducer and the bead capture strategy were performed at 65°C in standard 10 mm path-length quartz cells (estimated probed volume is 150 µL) on a custom-made detection platform described elsewhere [6]. Probe-grafted micro-beads were suspended in 0.1% Tween-20 aqueous solution with an excess of positive polymer (30 min/RT). Any unbound

polymer was removed by adequate washes. These "duplex beads" were introduced in the fluorescence cell (3 mL of pure water/65°C) to give approximately 10 beads in 200 µL. These particular conditions have shown an exceptional ability to allow hybridization and also to increase the stringency of the medium [12] Detailed protocols can be found elsewhere [8].

On-bead fluorescence detection on µEMT measurements were done with 25 µL droplets of target+duplex beads mixture (500 beads/µL) deposited on the electro-magnetic trap.

3 RESULTS

3.1 Influence of the bead size on magnetic trapping efficiency

Superparamagnetic particles are particles that have no permanent magnetic moment but can be momentarily magnetized when exposed to an external magnetic field. If this magnetic field is spatially non-uniform, the presence of a magnetic field gradient results in a magnetic force exerted on the magnetic particle. Given the external magnetic field H, the magnetic force (F_{mag}) on a bead can be estimated by Eq. 1 [13]:

$$\vec{F}_{mag} = \frac{2}{3}\chi V_p (\vec{H}.\nabla)\vec{B} = \frac{2}{3}\frac{\chi V_p}{\mu_0}\nabla B^2 \tag{1}$$

where χ is the magnetic susceptibility of the particle, V_p its volume.

In microfluidic flow environment, in addition to the magnetic force, the magnetic particles are subjected at the same time to a hydrodynamic drag force (we assumed the gravitational force negligible), which is described by Stoke's Law:

$$\vec{F}_{hydro} = 6\pi\eta R.\vec{v}_f \tag{2}$$

where η is the solvent viscosity (here, we used water η = $8.9.10^{-4}$ Nm.s^{-2}), R is the radius of the particle, v_f is the fluid velocity. Combining equation (1) with (2), we obtain:

$$v_f < \frac{4}{27}\frac{\chi R^2}{\mu_0 \eta}\nabla B^2 \tag{3}$$

Equation (3) gives the maximum fluid velocity, and consequently the maximum bead velocity (v_{max}) for which the condition $F_{mag} > F_{hydro}$ is realized, i.e. when the magnetic beads can be captured and magnetically confined against the the hydrodynamic force.

Magnetic field profiles created by microfabricated electromagnetic traps and the resulting magnetic forces exerted on the superparamagnetic beads have been simulated using finite-element analysis (Comsol 3.2). When a current of 300 mA is flowing through the gold wire, a

magnetic field peak of 2 mT is achieved at the center of the 1st generation of μEMT, above the PDMS layer. The addition of the nickel micropost in the center of the μEMT (2nd generation) increases the magnetic field peak at 6 mT. Fig. 2 shows the simulated profiles for magnetic force exerted on 2.8 μm superparamagnetic beads for the two designs of μEMT. As expected, the second generation of μEMT gives a theoretical magnetic force of almost one order of magnitude higher that in the case of the first generation.
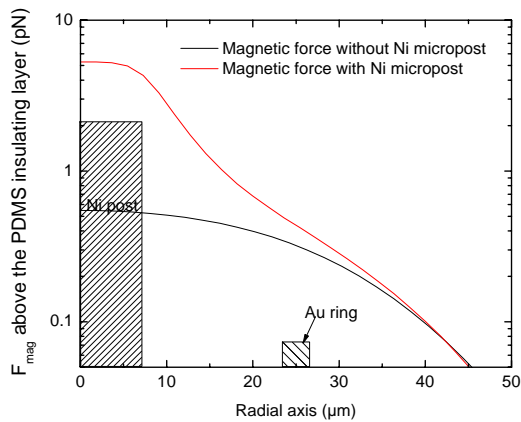

Fig. 2: Magnetic force profile in a cylindrical geometry, for both μEMT designs (with or without the Ni micropost)

This is in agreement with the experimental observations presented in table 1, which gives the experimental maximum averaged bead velocity (v_{max}) in order to trap 100 % of the beads flowing in a microfluidic channel, above the μEMT (i.e. when the condition for v_{max} from Eq. 3 is met). These experimental bead velocities were determined using particle tracking motion software. In the case of 2.8 μm beads (first row in table 1), we can see that the maximum bead velocity allowed is ~ 4 times higher when using the 2nd generation of μEMT instead of the 1st one (without the nickel micropost). This new design then gives us the possibility of speeding up the flow rates in microfluidic channels (thus reducing the time for a sample to be analyzed) without affecting the efficiency of the magnetic bead capture in a microscopic volume suitable for the optical detection (see next section).

Bead size (μm)	volume susceptibility	1st generation speed (μm.s^{-1})	2nd generation speed (μm.s^{-1})
2.8	0.7	7	30
1	1.4	-	35
0.5	0.4	-	5

Table 1: Maximum average velocity (v_{max}) of magnetic beads with different sizes, allowing 100 % trapping efficiency in a microfluidic channel for the both μEMT designs.

It is expected that the decrease of the particle size should strongly reduce the magnetic force F_{mag} as it scales as $\propto R^3$, while the hydrodynamic one (F_{hydro}) scales as $\propto R$. This point is well illustrated when comparing the maximum velocity v_{max} that still allow to trap 100 % of the 2.8 μm beads ($v_{max}\sim 30$ μm.s^{-1}) which is higher than the one obtained when using 0.5 μm beads ($v_{max}\sim 5$ μm.s^{-1}) (both types of particles having comparable magnetic susceptibilities).

3.2 Influence of the bead size on optical detection

Fluorescence emission from magnetically immobilized beads was collected by a custom-made confocal microscope optimized for polymeric transducer excitation and emission. For this series of experiments in static mode (no macroscopic fluid flow), a suspension of triplex-grafted magnetic beads was first deposited on the μEMT chip. A current of 300 mA was then applied to the μEMT during 5 minutes to trap the magnetic beads and the fluorescence signal was then acquired during a 2D scan across the μEMT center. During data acquisition, current is lowered to 50 mA to maintain beads in place (but avoids further trapping). A brightfield image was also acquired (see fig. 3a) in order to evaluate the number of beads captured during each experiment and normalize the fluorescence intensity to the number of beads captured (fig. 3b).
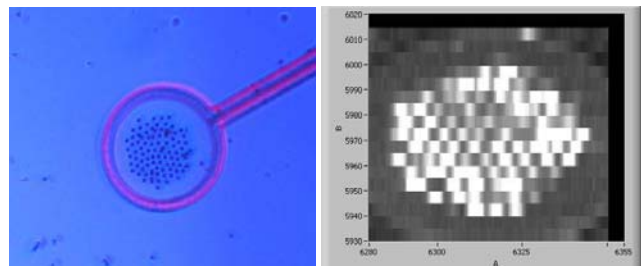

Fig. 3: (a) Bright field image and (b) fluorescence image of bead capture on a first generation of μEMT.

Figure 4 shows the linear relationship between luminescence intensity and triplex surface coverage of magnetic captured beads in the center of a 1st generation μEMT. Base on this we can extrapolate a limit of detection of 7.5 copies / μL or 150 target molecules by bead. Higher standard deviation value on blank leads to higher LOD mainly due to the nature of medium surrounding the analyzed beads.

As opposed to optical detection in homogeneous aqueous media, the background signal from a solid substrate such as a multilayer-built chip is tricky to control. Negative control was done using a target having a single sequence mismatch ("single nucleotide polymorphism", SNP). A behavior similar to that observed for homogenous detection experiments was noted, albeit with a slight increase in fluorescence signal. Once again, discrimination

between perfect match (square, figure 4) and single mismatch (triangle, figure 4) can be done at very low target concentrations, with a good contrast signal (around 5) between specific detection and SNP.
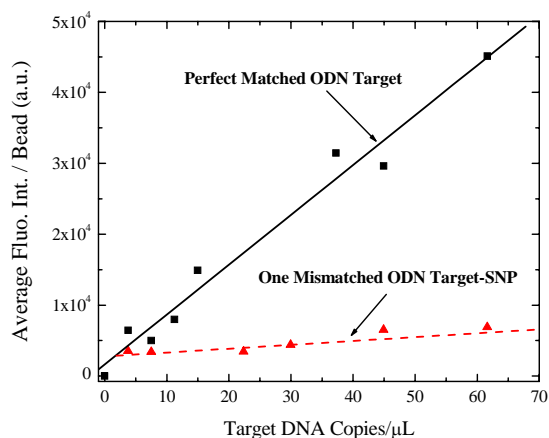

Fig. 4: Confocal fluorescence measurement of triplex beads captured by µEMT. Calibration curve for on-beads detection of 20-mer oligonucleotides target analyte revealed by polymer over 20-mer capture probe sequence

The use of particles having a diameter significantly smaller than the excitation source should minimize fluorescence and scattered background. On-bead detection in suspension, with magnetic beads diameter varying from 2.8 µm to 500 nm, was investigated using the custom-made fluorometer described previously. Detection was performed by monitoring the increased fluorescence emission (at 530 nm) that followed the addition of ssDNA targets to a suspension of duplex-grafted beads (~8 beads in the probed volume of 150 µL, ~10^6 duplex species/bead). The calibration curve for the 2.8 µm diameter beads was found to be linear up to 100 DNA copies/µL, with a calculated LOD of 1.4 copies/µL. Interestingly, as shown in Table 2, the concentration-dependent fluorescence is increasing by 6 when bead diameter is decreased from 2.8 µm to 500 nm. As expected, by decreasing the particle size, the fraction of the scattered light contribution to the measured fluorescence signal is reduced, leading to a higher signal/noise ratio and a better sensitivity of the system.

Bead size (µm)	Concentration-dependent fluorescence (Fluo.(a.u.)/copy/µL)	Background Signal (a.u.)
2.8	1150	1.05×10^5
1	4760	6.5×10^4
0.5	6050	3.5×10^4

Table 2: In-suspension fluorescence data for 3 different magnetic beads sizes

4 CONCLUSION

In conclusion, this study shows that direct on-bead detection of target ssDNA at the center of a micro-electromagnetic traps (µEMT) offers high sensitivity and selectivity. A systematic investigation of particle mobility under magnetic field and fluorescence signal (S/N ratio) was performed as a function of the magnetic bead size ranging from 2.8 to 0.5 µm, using a novel and more performing design of µEMT, integrated in a microfluidic platform. We have shown that while reducing the size of magnetic particles offers higher sensitivity for the optical detection, it also reduces the magnetic trapping efficiency and the dynamic range for the microfluidic flow. While the work in progress is aimed to determine the best compromise between the sensitivity and trapping efficiency, these results demonstrate the possibility to detect DNA targets with an unprecedented sensitivity and selectivity and open the way for the development of complex analytical point-of-care diagnostics and field analysis systems based on this principle.

REFERENCES

[1] Wang J., Anal.Chim.Acta, 500, 247-257, 2003
[2] Katz E, Willner I., Angew. Chem. Int. Ed., 43, 6042, 2004.
[3] Ramadan Q., Samper V., Poenar D., Yu C., J. Magn. Magn. Mater., 281, 150, 2004.
[4] Choi J.W., Liakopoulos T.M., Ahn C.H., Biosensors & Bioelectronics, 16, 409, 2001.
[5] Lee C.S., Westervelt R.M., Appl. Phys. Lett., 79(20), 3308, 2001.
[6] Doré K., Dubus S., Ho H-A., Lévesque I., Brunette M., Corbeil G., Boissinot M., Boivin G., Bergeron M.G., Boudreau D., Leclerc M., J. Am. Chem. Soc. 126, 4240, 2004.
[7] Dubus S., Gravel, J.-F. Le Drogoff B., Veres T., Boudreau D., Anal. Chem, submitted, 2006.
[8] Dubus S., Gravel J.-F., Le Drogoff B., Veres T., Boudreau D., Biosensors & Bioelectronics, submitted, 2006.
[9] Le Drogoff B., Dubus S., Gravel J.-F., Boudreau D., Veres T., in preparation, 2006.
[10] Xia Y., Whitesides G.M., Angew. Chem. Int. Ed., 37, 550. 1998.
[11] Ho H-A, Boissinot M., Bergeron M.G., Corbeil G., Doré K., Boudreau D., Leclerc M., Angew. Chem. Int. Ed. 41, 1548, 2002.
[12] Ho H.-A., Doré K., Boissinot M., Bergeron M.G., Tanguay R.M., Boudreau D., Leclerc M., J. Am. Chem. Soc. 127, 12673, 2005
[13] Bagster D.F., Int. J. Mineral Proc., 10, 1, 1987.